

Mechano-chemical activation synthesis (MCAS) of nanocrystalline magnesium alanate hydride $[\text{Mg}(\text{AlH}_4)_2]$ and its hydrogen desorption properties

R.A. Varin^{a,*}, Ch. Chiu^a, T. Czujko^a, Z. Wronski^{a,b}

^a Department of Mechanical Engineering, University of Waterloo, Waterloo, Ontario, Canada N2L 3G1

^b Materials Technology Laboratory, CANMET, Natural Resources Canada, 568 Booth Street, Ottawa, Ontario, Canada K1A 0G1

Received 5 July 2006; received in revised form 21 August 2006; accepted 21 August 2006

Available online 22 September 2006

Abstract

A successful synthesis of the $\text{Mg}(\text{AlH}_4)_2 + 2\text{NaCl}$ mixture by the mechano-chemical activation synthesis (MCAS) for 5 and 10 h has been achieved. The nanocrystalline $\text{Mg}(\text{AlH}_4)_2$ hydride in the mixture has the grain size on the order of 18 nm. Even relatively short milling for just 10 h seems to result in a partial decomposition of the initially formed $\text{Mg}(\text{AlH}_4)_2$ into the nanocrystalline $\beta\text{-MgH}_2$, elemental Al (grain size ~ 26 nm) and hydrogen gas. A number of DSC tests at the scan rate of $4^\circ\text{C}/\text{min}$ of the $\text{Mg}(\text{AlH}_4)_2 + 2\text{NaCl}$ mixture synthesized for 5 and 10 h show either endothermic or exothermic heat flow changes at the $\sim 125\text{--}180^\circ\text{C}$ range due to the decomposition of $\text{Mg}(\text{AlH}_4)_2$. Endothermic peaks with the maxima at ~ 271 and 316°C due to the decomposition of $\beta\text{-MgH}_2$ and the formation of Al_3Mg_2 intermetallic as well as $\text{Al}(\text{Mg})$ solid solution are present. The peak at $\sim 452^\circ\text{C}$ is due to the eutectic melting of the Al_3Mg_2 and $\text{Al}(\text{Mg})$ mixture. Prolonged milling for 40 h results in a complete decomposition of the $\text{Mg}(\text{AlH}_4)_2$ into two nanocrystalline solid phases such as $\beta\text{-MgH}_2$ (grain size ~ 11 nm) and the elemental Al (grain size ~ 20 nm), and hydrogen gas. DSC tests at the scan rate of $4^\circ\text{C}/\text{min}$ up to 500°C of the 40 h milled powder, which contains $\beta\text{-MgH}_2$, results in two endothermic peaks with the maxima at $\sim 292^\circ\text{C}$ due to the decomposition of $\beta\text{-MgH}_2$ and $\sim 452^\circ\text{C}$ due to the eutectic melting. TGA tests for the 5 and 10 h milled sample give the total weight loss of ~ 2.45 and 2.16 wt.%, respectively. The hydrogen desorption kinetics of the as-synthesized powders directly after milling were also evaluated using a Sieverts-type apparatus.
© 2006 Elsevier B.V. All rights reserved.

Keywords: Hydrogen storage; Nanostructured materials; Complex hydrides; Magnesium alanate; Mechano-chemical activation synthesis; Reactive milling; X-ray diffraction; Differential scanning calorimetry; Hydrogen desorption kinetics

1. Introduction

Hydrogen storage in solid hydrides is the most attractive method of on-board hydrogen storage for fuel cell powered passenger vehicles [1–3]. Hydrogen storage targets established for 2010 and 2015 by the FreedomCAR program [1] clearly show that only hydrides with the gravimetric hydrogen storage capacities higher than 6 wt.% are viable for potential commercial automotive application. So far, the only group of hydrides which have both high volumetric and gravimetric hydrogen densities meeting the targets are complex metal hydrides having a mixed ionic-covalent bonding between metal and hydrogen complex

[4,5]. Among them, a potentially attractive complex hydride is the magnesium tetrahydroaluminate (magnesium alanate) $\text{Mg}(\text{AlH}_4)_2$. Its theoretical hydrogen capacity is 9.3 wt.% and the hydride is based on two inexpensive light metals Mg and Al. This hydride was first synthesized by chemical methods over 50 years ago and then thoroughly investigated by Ashby et al. [6] and more recently investigated by Fichtner et al. [7–9], Schwarz et al. [10] and Fossdal et al. [11,12] who found that it decomposes in two major steps with the first step around 160°C in which three quarters of the bound hydrogen was released. This relatively low dehydrogenation temperature of the first step is attractive enough to warrant further studies.

Extensive research in the last decade led to a rather strong consensus that nanocrystalline solid hydrides, specifically obtained by mechanical milling in various types of ball mills and characterized by the existence of nanometric grains within the

* Corresponding author. Fax: +1 519 888 6197.

E-mail address: ravarin@mecheng1.uwaterloo.ca (R.A. Varin).

hydride particles, exhibit substantially enhanced hydrogenation/dehydrogenation properties [5,13,14]. Our recent attempt of a direct mechano-chemical synthesis of nanocrystalline $\text{Mg}(\text{AlH}_4)_2$ by controlled reactive mechanical alloying [15] has been unsuccessful due to accelerated formation of the $\text{Al}(\text{Mg})$ solid solution which, most likely, inhibited the reaction of MgH_2 , Al and H_2 to form $\text{Mg}(\text{AlH}_4)_2$.

However, an alternative indirect method of the synthesis of $\text{Mg}(\text{AlH}_4)_2$ is the mechano-chemically activated metathesis reaction [16,17]. Mamatha et al. [18,19] subjected a mixture of NaAlH_4 and MgCl_2 to ball milling for 3 h (Retsch ball mill) and obtained a mixture of synthesized $\text{Mg}(\text{AlH}_4)_2$ and NaCl . Subsequent DSC analysis of the mechano-chemically prepared powders showed three endothermic peaks with maxima around 140, 270 and 450 °C, which were interpreted as corresponding to the decomposition of $\text{Mg}(\text{AlH}_4)$ into MgH_2 , Al and H_2 , decomposition of MgH_2 into Mg and formation of Al_3Mg_2 , and eventually melting of Al_3Mg_2 and Al mixture, respectively. Kim et al. [20] synthesized a mixture of $\text{Mg}(\text{AlH}_4)$ and NaCl after 1 h in a Spex 8000 ball mill. DSC test was carried out only up to slightly over 300 °C and showed the first exothermic peak at the range of 115–150 °C and the second endothermic peak at the range of 240–290 °C. They concluded that the first exothermic reaction corresponds to the decomposition of $\text{Mg}(\text{AlH}_4)$ into MgH_2 , Al and H_2 and the second endothermic peak to the decomposition of MgH_2 . Apparently, there is a clear controversy between the results of Mamatha et al. [18,19] who report endothermic and those of Kim et al. [20] who report exothermic reaction for the decomposition of $\text{Mg}(\text{AlH}_4)$.

The objective of this work is two-fold. First, to study the effect of the milling time longer than 3 h on the microstructural development of the initial mixture of NaAlH_4 and MgCl_2 and the

formation of $\text{Mg}(\text{AlH}_4)$ and NaCl mixture. Second, to clarify the thermal events occurring during DSC analysis of the synthesized mixture of $\text{Mg}(\text{AlH}_4)$ and NaCl with a special emphasis on the heat flow event in the range of 115–150 °C.

2. Experimental

As-received NaAlH_4 (90% purity; Sigma–Aldrich) and anhydrous MgCl_2 (99% purity; Alfa–Aesar) were mixed together in the 2:1 stoichiometric ratio (corresponding wt.% of NaAlH_4 and MgCl_2 in the mixture are 53.1 and 46.9 wt.%, respectively, so as a result the weight ratio is ~ 1.13 g NaAlH_4 :1 g MgCl_2). Subsequently, the mixture was subjected to controlled mechanical milling under 600 kPa pressure of high purity argon (99.999% purity) in the magneto-mill Uni-Ball-Mill 5 (A.O.C. Scientific Engineering Pty Ltd., Australia) [21–23]. Two Nd–Fe–B super-strong magnets at 6 and 8 o'clock positions with WD = 10 and 2 mm, respectively, were used (Fig. 1) (WD, working distance between the vial and the magnet). Four hardened steel balls in the milling vial yielded the ball-to-powder weight ratio of 40:1. The samples were milled continuously for 5, 10 and 40 h at 225 rpm.

Morphological examination of powders was conducted with a high-resolution, field emission gun SEM (FEG SEM) LEO 1530 equipped with integrated EDAX Pegasus 1200 EDS/OIM. The size measurement of the powder particles for various samples was carried out by attaching loose powder to the sticky carbon tape and taking pictures under secondary electron (SE) mode in SEM. The images were analyzed by the Image Tool v.3.00 software. The size of the powders were calculated as the particle equivalent circle diameter, $\text{ECD} = (4A/\pi)^{1/2}$, where A represents the projected particle area.

The crystalline structure of the as-milled powders was characterized by Bruker D8 powder diffractometer using $\text{Cu K}\alpha$ (not monochromated) radiation at the scan range from 20° to 90°, step size of 0.05°/s, accelerating voltage of 40 kV and a current of 30 mA. The nanograin (crystallite) size of phases residing in the milled powders was calculated from the broadening of their respective XRD peaks. Since the Bragg peak broadening in an XRD pattern is due to a combination of grain refinement (nanograin/crystallite) and lattice strains, it is customary to use computing techniques by means of which one can separate these two contributions. The separation of crystallite size and strain was obtained from Cauchy/Gaussian approximation by the linear regression plot according to

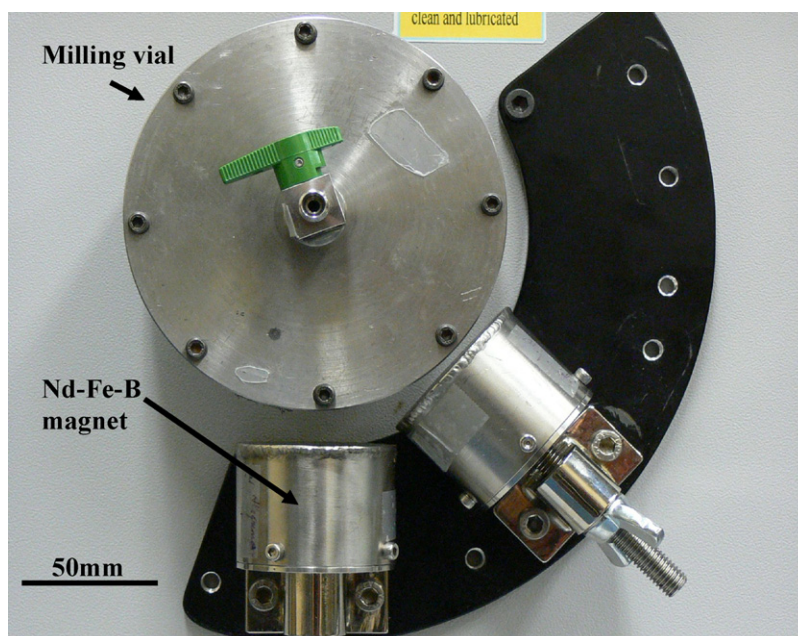


Fig. 1. Angular positions of Nd–Fe–B super-strong magnets at 6 and 8 o'clock for ball milling under high-energy impact mode (IMP68) in the Uni-Ball-Mill 5. The angular positions of external magnets can be changed at each of the controlled modes of milling [21–23].

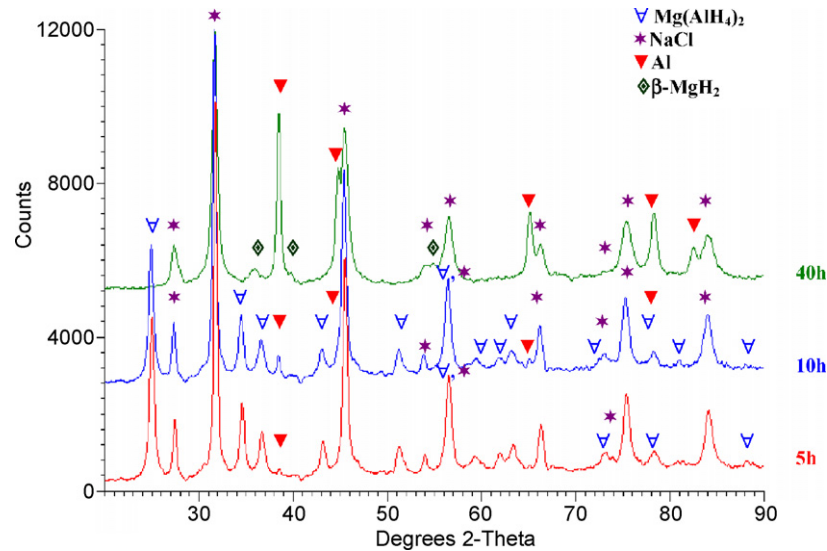


Fig. 2. The XRD patterns of the initial mixture of NaAlH₄ and MgCl₂ powders after milling for 5, 10 and 40 h.

the following equation [24]:

$$\frac{\delta^2(2\theta)}{\tan^2\theta} = \frac{K\lambda}{L} \left(\frac{\delta(2\theta)}{\tan\theta \sin\theta} \right) + 16e^2 \quad (1)$$

where the term $K\lambda/L$ is the slope, the parameter L is the mean dimension of the nanograin (crystallite) composing the powder particle, K is constant (~ 1); e the so-called “maximum” microstrain (calculated from the intercept); λ the wave length; θ is the position of the analyzed peak maximum. The term $\delta(2\theta) = B[1 - (b^2/B^2)]$ (rad) is the instrumental broadening-corrected “pure” XRD peak profile breadth [24], where B and b are the breadths in radians of the same Bragg peak from the XRD scans of the experimental and reference powder, respectively. They were calculated by the software Traces™ v.6.5.1 as the full-widths at half maximum, FWHM, after $K\alpha_2$ stripping. A compound LaB₆, the National Institute of Standards and Technology (NIST) standard reference material (SRM) 660 was used as a reference for subtracting the instrumental broadening from FWHM. It must be noted that when the FWHM of the instrumental line profiles were obtained in this manner, the Bragg peaks for the LaB₆ SRM were at different 2θ angles than those of the analyzed phases in the milled powders. The interpolated FWHM values between angles for the SRM peaks were found using a calibration curve.

Differential scanning calorimetry (DSC) was performed on a Netzsch 404 instrument using ~ 20 mg of a sample heated in an alumina crucible at the scan rate of 4 and 20 °C/min, and a 50 ml/min Ar flow rate. Thermogravimetric analysis (TGA) was performed on a TA INSTRUMENT Q600 instrument using ~ 10 mg of a sample heated at a heating rate of 4 °C/min under a 100 ml/min nitrogen gas flow rate. All samples were tested almost immediately after completion of milling to avoid aging phenomena due to hydrolysis of MgH₂ [25].

The hydrogen desorption kinetics of the as-synthesized powders directly after milling were also evaluated using a Sieverts-type apparatus custom-built by A.O.C. Scientific Engineering Pty Ltd., Australia (see Fig. 2 in Ref. [26]). The weight of the powder sample in the kinetics experiments was ~ 100 – 150 mg. The calibrated accuracy of desorbed hydrogen capacity is about ± 0.2 wt.% H₂ and that of temperature reading ± 5 °C. Before starting the desorption test, the inner tubing of the apparatus was also evacuated and purged four times with argon and then two times with hydrogen. Subsequently, hydrogen under pressure of 41 bars was admitted into the airtight cylindrical desorption chamber containing the hydride powder and the temperature of the chamber was gradually increased up to the desired desorption temperature. The 41 bar pressure barrier was applied to prevent any desorption during the period of temperature stabilization (15–20 min) within the desorption chamber. Once the temperature was stabilized the hydrogen pressure was quickly reduced to 0.1 MPa and the hydrogen desorption process was monitored. No elaborate activation procedure was applied to the powders.

3. Results and discussion

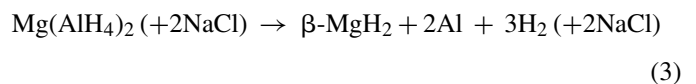
3.1. Microstructure of synthesized powders after milling

Mean ECD values for the particles of the powders after milling for 5, 10 and 40 h are 2.7 ± 2.3 , 2.4 ± 2.2 and 2.3 ± 2.2 μm , respectively. EDS analysis has shown that the distribution of Mg, Al, Na and Cl is homogeneous in all the powders.

The XRD pattern in Fig. 2 shows the presence of Mg(AlH₄)₂ (identified from JCPDS # 47-980) and NaCl (identified from JCPDS # 05-0628) after milling for 5 and 10 h. It can be assumed that after 5 h of MCAS the synthesis of Mg(AlH₄)₂ is completed according to the following reaction:



as also reported by Mamatha et al. [18,19] and Kim et al. [20]. After milling for 5 h only a single, very weak XRD peak of elemental Al is recognizable in the XRD pattern (Fig. 2; at $2\theta \sim 38^\circ$). Increasing the milling duration to 10 h results in the appearance of more Al peaks and one or two very weak peaks of β -MgH₂ (Fig. 2). After 40 h, the peaks of Mg(AlH₄)₂ disappear while the well-discerned peaks of β -MgH₂ and Al appear. The pressure inside the milling cylinder increased by ~ 465 kPa from which one can estimate that ~ 2.5 wt.% of H₂ was desorbed during milling for 40 h. It is clear that initially, the mixture of Mg(AlH₄)₂ and 2NaCl is being formed but subsequently, during further prolonged milling, there is a gradual decomposition of Mg(AlH₄)₂ according to



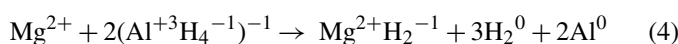
It is to be pointed out that in the present work the decomposition of Mg(AlH₄)₂ upon milling occurs without the addition of Ti metal catalyst, which was used by Mamatha et al. [19] to induce similar reaction.

Table 1

Grain (crystallite) size, L , and lattice strain, e , of the phases in the powders after milling for 5, 10 and 40 h as estimated from Eq. (1)

Milling time (h)	Phase	Nanograin (crystallite) size, L (nm)	Lattice strain, e	R^2	No. of XRD peaks
5	Mg(AlH ₄) ₂	18	0	0.973	11
10	Mg(AlH ₄) ₂	18	6.6×10^{-4}	0.975	9
10	Al	26	0	0.995	4
40	Al	20	0	0.945	4
40	β -MgH ₂	11	0	0.983	3

As opposed to the reaction (2), which occurs during short milling, the reaction (3) is not a metathesis reaction. Instead, a long milling triggers a reduction–oxidation (redox) reaction. Indeed, the H and Al are mutually oxidized and reduced as shown below:



and the partial reactions are as follows:



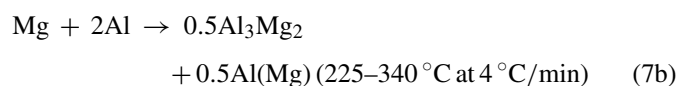
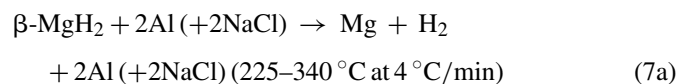
Nanocrystalline Mg(AlH₄)₂ with the grain size of ~ 18 nm (Table 1) is produced after MCAS for 5 and 10 h in excellent agreement with Mamatha et al. [19]. Grain sizes of Al (~ 20 nm) and β -MgH₂ (~ 11 nm) after decomposition of Mg(AlH₄)₂ during a prolonged milling for 40 h are still in a nanometric range (Table 1). However, it must be noted that with cycling, the complex hydrides generally may not maintain a small crystallite size.

3.2. DSC and TGA thermal analysis up to 500 °C

The NaCl by-product of the reaction (2) was not removed from the powders milled for 5 and 10 h because it does not react with Mg(AlH₄)₂ during heating and removing salt using chemical methods might bring impurities, which may affect the thermal behavior of Mg(AlH₄)₂ [20].

DSC traces registered at the scan rate of 4 and 20 °C/min for the powders milled for 5 and 10 h exhibit some small heat flow fluctuations at the low-temperature range of 125–180 °C (Fig. 3a and b) while the DSC trace for the 40 h milled powder is rather flat at this low-temperature range. These low-temperature thermal events will be discussed in more detail in Section 3.3. DSC traces registered at the scan rate of 4 °C/min clearly show two endothermic peaks for the 5 and 10 h milled powders at the 225–340 °C range and one endothermic event at a 450–460 °C range (Fig. 3a). As expected, increase of the scan rate to 20 °C/min shifts the medium-temperature range peak maxima to higher temperatures (~ 250 – 375 °C) but does not change the shape of the peaks (Fig. 3b). In order to analyze the nature of the thermal events observed in Fig. 3a above 180 °C the powder milled for 10 h which contains Mg(AlH₄)₂ was analyzed by running small samples of this powder in DSC at 4 °C/min to the temperatures marked by the vertical lines in Fig. 3c. The corresponding XRD patterns are shown in Fig. 4. After heating to 180 °C the only phases existing in the microstructure are residual NaCl, β -MgH₂ and the elemental Al confirming the decompo-

sition of Mg(AlH₄)₂ into β -MgH₂ and the elemental Al. The XRD peaks of decomposition product β -MgH₂ in Fig. 4 are rather weak since the amount of β -MgH₂ is small (in the reaction (2) there is only 1 mol of Mg(AlH₄)₂ per 2 mol of NaCl). After a DSC run to the temperature of 295 °C, higher than the temperature of the first DSC peak maximum at ~ 271 °C, the microstructure consists of residual NaCl, a negligible amount of β -MgH₂, small amount of Al₃Mg₂ intermetallic (very low peak intensities in Fig. 4) and large amount of Al(Mg) solid solution (high intensity XRD peaks in Fig. 4). Apparently, around the 271 °C peak the majority of β -MgH₂ decomposes in the endothermic reaction into free Mg and H₂. Simultaneously, reactions of Mg and Al to form Al₃Mg₂ and Al(Mg) solid solution must have occurred. The reactions can be written as follows:



After DSC run up to the temperature of 350 °C, which is higher than the temperature of the second DSC peak maximum at ~ 316 °C (Fig. 3c), the decomposition of the remnant MgH₂ is completed and the microstructure consists of residual NaCl, large amount of Al₃Mg₂ intermetallic compound (high intensity XRD peaks in Fig. 4) and large amount of Al(Mg) solid solution (high intensity XRD peaks in Fig. 4). As such, two endothermic peaks at ~ 271 and ~ 316 °C might arise either due to the decomposition of β -MgH₂ and the formation of the Al₃Mg₂ intermetallic compound or alternatively, due to the two-step decomposition of β -MgH₂ although the latter is not so clear.

It must be pointed out that the formation of Al(Mg) solid solution in due course and after complete decomposition of MgH₂ observed by XRD in Fig. 4 was first identified by visible shifting of Al peaks to lower angles, with respect to their position for a pure Al in the XRD patterns of powders heated in DSC to 295, 350 and 425 °C (Fig. 4). Subsequently, the lattice parameters of Al(Mg) were calculated by the software TracesTM v.6.5.1 and are listed in Table 2. It is clear that the lattice parameter of Al in the powders milled for 10 h is much larger after annealing in DSC at 295, 350 and 425 °C than that of the as-milled and 180 °C annealed samples. The lattice expansion is consistent with the magnitude of the atomic radius of Al and Mg, which is 0.1432 and 0.1604 nm, respectively [27]. Similar effect of

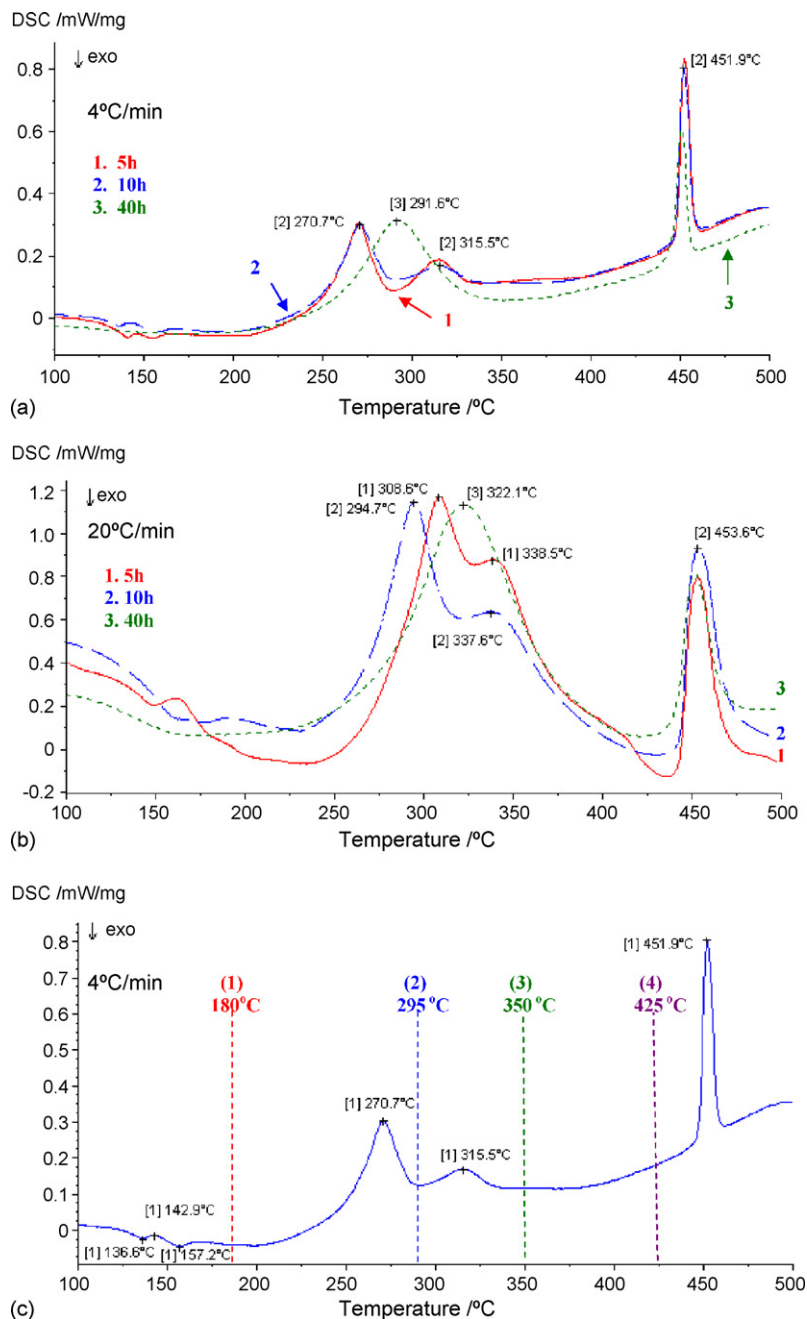


Fig. 3. DSC curves of powders after milling for 5, 10 and 40 h upon heating to 500 °C registered at the scan rate of: (a) 4 °C/min; (b) 20 °C/min; (c) the DSC curve of the powder after milling for 10 h showing a separation into the four segments corresponding to the thermal events registered on the curve (scan rate 4 °C/min).

the Al(Mg) solid solution formation during reactive milling of the elemental powders with Mg–2Al ratio, pre-alloyed Mg–2Al ingot and AZ91 alloy was reported in [15]. Fosdhal et al. [12] claimed the formation of the Al(Mg) solid solution during low-temperature desorption of $\text{Mg}(\text{AlH}_4)_2$ below 180 °C which is not confirmed in the present work (Fig. 4 and Table 2). Mamatha et al. [18,19] never reported the formation of the Al(Mg) solid solution although Kim et al. [20] mentioned about increase in the lattice parameter of Al most probably due to formation of the Al(Mg) solid solution. After heating to 425 °C the microstructure remains the same as that after the 350 °C annealing. The nature of the endothermic reaction at ~452–454 °C

upon heating (Fig. 3a–c) is due to the eutectic melting of the mixture of Al_3Mg_2 and Al(Mg) solid solution which essentially occurs according to the equilibrium phase diagram of Al–Mg as reported in [15].

In the DSC curve of powder after milling for 40 h, only a single endothermic peak due to the decomposition of $\beta\text{-MgH}_2$ and formation of Al_3Mg_2 and Al(Mg) is observed regardless of the scan rate (Fig. 3a and b). It is to be pointed out that the DSC run of the 40 h milled powder at the scan rate of 4 °C/min up to 350 °C which is above the peak maximum at ~292 °C in Fig. 3a, resulted in the formation of the mixture of Al_3Mg_2 and Al(Mg) solid solution whose lattice parameter is also listed

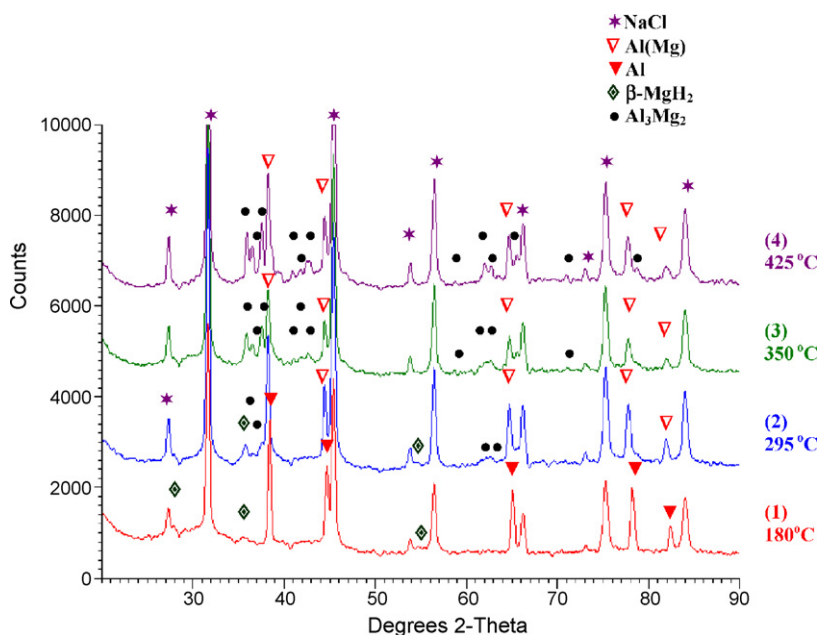


Fig. 4. XRD patterns corresponding to the powders heated to 180, 295, 350 and 425 °C in a DSC test shown in Fig. 3c.

in Table 2. This clearly confirms that the formation of Al_3Mg_2 and $\text{Al}(\text{Mg})$ in the present work occurs with the assistance of temperature rather than during ball milling as reported in [15]. This can be related to different methods of synthesis used in the present work (MCAS) and in [15] (reactive mechanical milling of elemental powders or alloys). Mamatha et al. [18,19] and Kim et al. [20] reported only a single endothermic peak with the maximum around 280–290 °C for the mixture $\text{Mg}(\text{AlH}_4)_2 + 2\text{NaCl}$. The peak at ~ 452 °C is due to the eutectic melting of the Al_3Mg_2 and $\text{Al}(\text{Mg})$ mixture.

The temperature ranges of two weight losses at ~ 120 – 170 °C range and ~ 270 – 300 °C, which were observed in TGA tests for the powders containing $\text{Mg}(\text{AlH}_4)_2$ (5 and 10 h) (not shown here), match well with those at DSC curves (~ 120 – 170 and ~ 225 – 340 °C ranges; Fig. 3c). The TGA weight losses in the first and second step decomposition for the 5 h milled powder are 2.37 and 0.08 wt.%, respectively. Corresponding weight losses for the 10 h milled powder are 2.14 and 0.02 wt.%. Assuming the MCAS is completed (i.e., products have a 1 mol of $\text{Mg}(\text{AlH}_4)_2$ and 2 mol of NaCl) (Fig. 2), the theoretical hydrogen capacity in the mixture of $\text{Mg}(\text{AlH}_4)_2 + 2\text{NaCl}$ is ~ 3.97 wt.% rather than

~ 9.3 wt.% as in a pure $\text{Mg}(\text{AlH}_4)_2$. From TGA analysis, the largest total weight loss ~ 2.45 wt.%, which is observed for the 5 h milled powder, is much less than the theoretical value of ~ 3.97 wt.%. A short of ~ 1.5 wt.% might be a combined effect of the partial decomposition of $\text{Mg}(\text{AlH}_4)_2$ during milling for 5 h and the underestimation of the weight loss in the second step (~ 270 – 300 °C) due to the oxidation of Mg during TGA run under flowing nitrogen. The total hydrogen desorption of only ~ 2.16 wt.% in TGA of the 10 h milled powder is most probably due to the prior partial decomposition of $\text{Mg}(\text{AlH}_4)_2$ during milling. No weight loss in the 100– 180 °C range for the 40 h milled powder further confirms that $\text{Mg}(\text{AlH}_4)_2$ is fully decomposed after a prolonged milling time.

3.3. The nature of low-temperature heat flow events in DSC

The heat flow effects due to the decomposition of $\text{Mg}(\text{AlH}_4)_2$ in DSC are difficult to monitor due to its very low enthalpy of decomposition [19] and corresponding small amount of heat flow (small DSC peaks). Fig. 5a shows the enlargement of the low-temperature region up to 180 °C observed on the full DSC curve in Fig. 3a (scan rate 4 °C/min) of the powder synthesized for 10 h. Taking the flat DSC portion for the 40 h sample as a baseline, one can invoke the existence of either two exothermic or one endothermic peaks due to the decomposition of $\text{Mg}(\text{AlH}_4)_2$. In order to shed more light on these low-temperature heat flow events, we tested a few powder samples milled for 5 and 10 h at the scan rate of 20 °C/min, which are plotted in Fig. 5b together with the flat trace for the 40 h sample, which can be considered as a baseline. With respect to this baseline, one 5 h and one 10 h milled samples show the DSC humps, which could be considered as endothermic events. In contrast, other 5 and 10 h samples show a diffuse trough that could be considered as an exothermic reaction. In

Table 2

Lattice parameters of Al and $\text{Al}(\text{Mg})$ solid solution in the as-milled and DSC tested samples

Milling time (h)	Temperature of DSC test (°C)	Lattice parameter of Al (FCC) (nm)
10	As-milled	0.4037 ± 0.0015
10	180	0.4039 ± 0.0015
10	295	0.4059 ± 0.0018^a
10	350	0.4062 ± 0.0016^a
40	350	0.4065 ± 0.0012^a
10	425	0.4063 ± 0.0013^a

^a $\text{Al}(\text{Mg})$ solid solution.

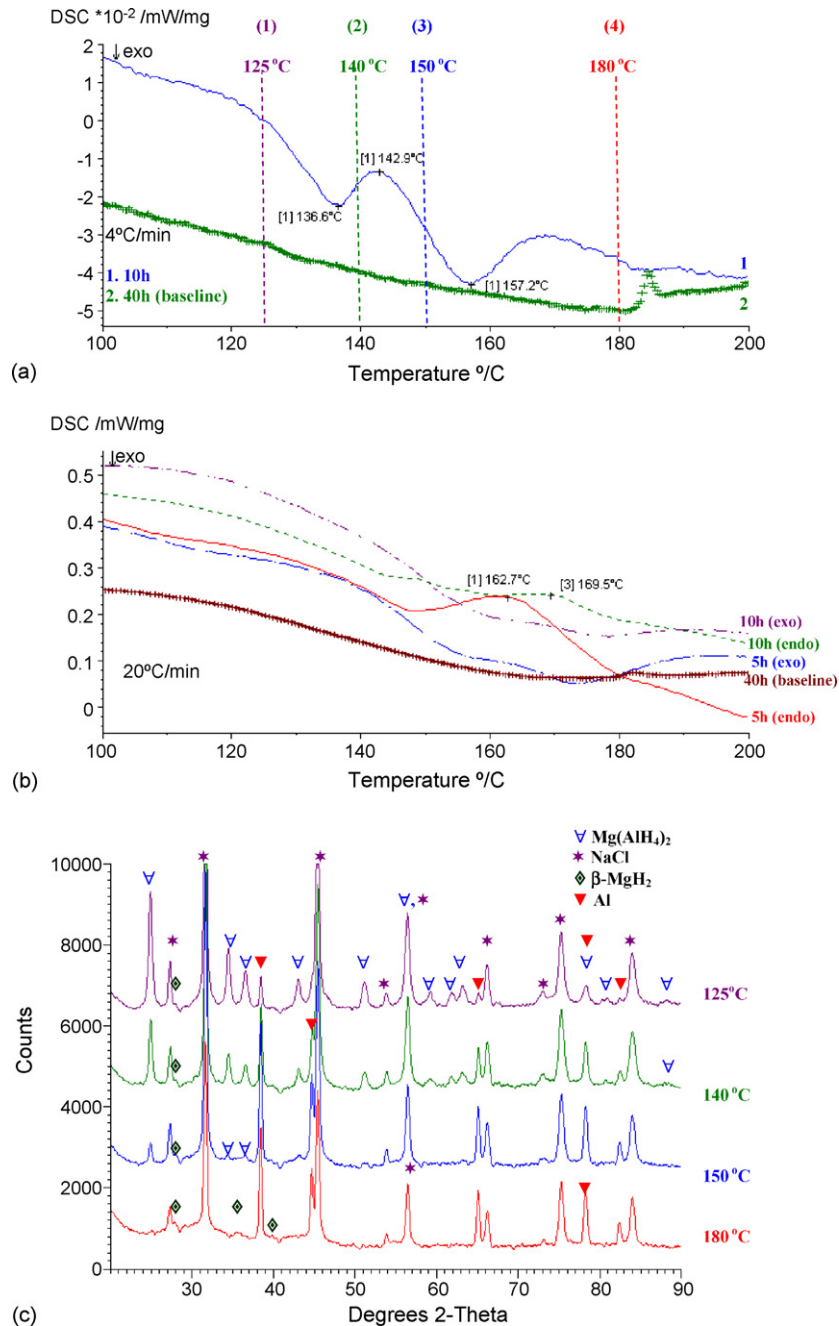


Fig. 5. An enlargement of the low-temperature section of DSC curve of the powders milled for 10 and 40 h registered at the scan rate of: (a) 4 °C/min; (b) 20 °C/min; (c) corresponding XRD patterns of the powders after heating to 125, 140, 150 and 180 °C in a DSC test.

order to investigate the nature of microstructural changes up to 180 °C a few samples of the 10 h milled powder which contains Mg(AlH₄)₂ were run in a DSC test at the scan rate of 4 °C/min up to the temperatures marked by the vertical lines in Fig. 5a. Subsequently, XRD phase analysis was performed for each sample after DSC test and the pertinent patterns are shown in Fig. 5c. Samples annealed to 125 and 140 °C still show the presence of Mg(AlH₄)₂, residual NaCl, traces of β-MgH₂ and the elemental Al rather than the Al(Mg) solid solution as mentioned earlier. This in essence is almost the same microstructure as that after ball milling for 10 h (Fig. 2). The presence of β-MgH₂ indicates that the beginning of the decomposition of

Mg(AlH₄)₂ starts occurring around 125 °C (scan rate 4 °C/min). After a DSC run up to 150 °C, the microstructure contains only a very small amount of Mg(AlH₄)₂ as can be deduced from a greatly reduced intensity of the strongest Mg(AlH₄)₂ peak at $2\theta \sim 25^\circ$ (100% intensity) and almost complete disappearance of two other strong peaks at $2\theta \sim 34.5^\circ$ (80% intensity) and $2\theta \sim 36.6^\circ$ (75% intensity) (JCPDS# 47-980) in Fig. 5c (150 °C). The absence of Mg(AlH₄)₂ after DSC run to 180 °C is an indication of its complete decomposition.

This analysis clearly shows that approximately up to 180 °C, Mg(AlH₄)₂ is already decomposed. However, the nature of this transformation as being either endothermic [18,19] or exother-

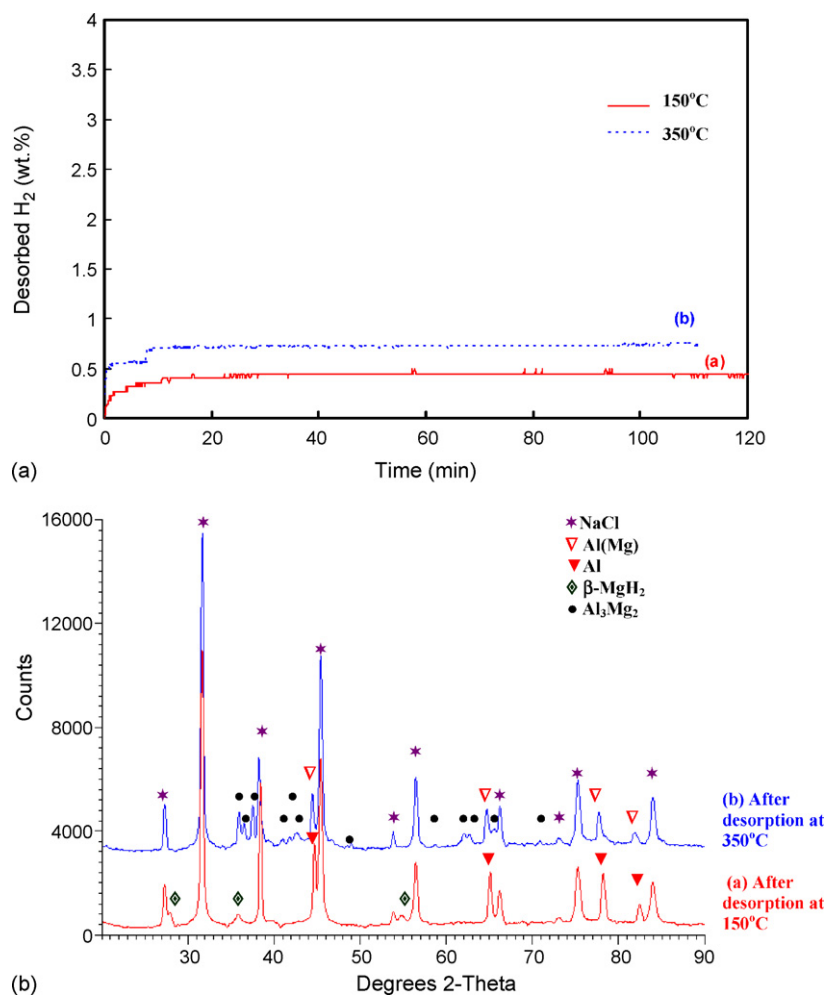


Fig. 6. (a) Hydrogen desorption kinetic curves obtained in a Sieverts-type apparatus at 150 and 350 °C of the $\text{Mg}(\text{AlH}_4)_2 + 2\text{NaCl}$ mixture synthesized for 5 h. (b) XRD of the powders desorbed at 150 and 350 °C.

mic [20] cannot be unambiguously established. Most probably, this situation arises owing to a very small enthalpy of decomposition of $\text{Mg}(\text{AlH}_4)_2$, which is cited in the literature as being equal to ~ 1.7 kJ/molH [19]. It is quite possible that at such small value of the enthalpy of decomposition, which in all practical terms is almost close to zero, even small microstructural fluctuations always present in the powders synthesized by mechano-chemical reactions may change the character of the decomposition reaction from endothermic [18,19] to exothermic [20].

3.4. Kinetics of desorption

Hydrogen desorption kinetics of the powder mixture $\text{Mg}(\text{AlH}_4)_2 + 2\text{NaCl}$ synthesized for 5 h were studied in a Sieverts-type apparatus at 150 and 350 °C (Fig. 6a). A hydrogen pressure barrier of 41 bar was supposed to prevent desorption before the system temperature was stabilized at the desired test temperature. The desorbed amounts of hydrogen at 150 and 350 °C are 0.45 and 0.75 wt.%, respectively. XRD patterns of the powder after desorption at 150 °C indicate a complete first step decomposition (reaction (3)) of $\text{Mg}(\text{AlH}_4)_2$ (Fig. 6b). How-

ever, the value 0.45 wt.% is much smaller than ~ 2.37 wt.% H_2 of the first step desorption estimated by TGA and much smaller than the theoretical value of ~ 2.98 wt.% H_2 resulting from the reaction (3) (the theoretical hydrogen capacity is ~ 3.97 wt.% in the mixture of $\text{Mg}(\text{AlH}_4)_2 + 2\text{NaCl}$, which is equal to the amount stored within four H_2 in $\text{Mg}(\text{AlH}_4)_2$; as a result, one H_2 should give us ~ 0.99 wt.% ($=3.97/4$) in the mixture; taking into account that three H_2 are desorbed in the reaction (3) and one H_2 is released in the reaction (7a), the theoretical amount of hydrogen desorbed in the reactions (3) and (7a) are ~ 2.98 and ~ 0.99 wt.%, respectively). The phase make up after desorption at 350 °C (Fig. 6b) confirms that both the Al_3Mg_2 intermetallic and Al(Mg) solid solution always form side by side when desorption is carried out above about 180 °C as discussed earlier in the text. The observed microstructure also indicates that at the temperature of 350 °C the hydrogen desorption was completed, i.e. both reactions (3) and (7) occurred. However, the desorbed value of 0.75 wt.% H_2 is still much smaller than the total ~ 2.45 wt.% H_2 desorbed in TGA and ~ 3.97 wt.% H_2 of the total amount of H_2 stored in the $\text{Mg}(\text{AlH}_4)_2 + 2\text{NaCl}$ mixture.

The question therefore arises as to the possible cause of incomplete desorption in a Sieverts-type apparatus. Fichtner et

al. [7] reported the equilibrium pressure of pure $\text{Mg}(\text{AlH}_4)_2$ in the 75–95 °C range to be between 88 and 130 bar. As a result, a hydrogen pressure barrier of 41 bar, which we used during temperature stabilization period in a Sieverts-type apparatus in the present work might have been insufficient to prevent the reaction (3) to occur during heating to 150 and 350 °C in the temperature stabilization period, giving rise to some desorption according to the reaction (3) even before the temperature was fully stabilized. This explanation is supported by the pressure increase monitored during temperature stabilization period at 150 °C. Since the pressure increase is due to two factors such as temperature and hydrogen release then its increment due to just hydrogen release can be estimated by subtracting the pressure increase due to temperature estimated from the heating of empty crucible from the pressure registered while heating crucible containing a powder sample synthesized for 5 h. This estimate gives ~ 1.79 wt.% H_2 already released during temperature stabilization period at 150 °C. Therefore, the total amount of hydrogen desorbed will be the sum of the hydrogen desorbed during temperature stabilization period (~ 1.79 wt.%) and the hydrogen desorbed in the isothermal desorption period of the test at 150 °C, i.e. 0.45 wt.%. This summation gives the total of 2.24 wt.% H_2 desorbed at 150 °C, which is still slightly smaller than the theoretical 2.98 wt.% H_2 .

Similar estimate taking into account the pressure increase calculated from the heating of empty crucible up to 350 °C gives ~ 2.5 wt.% H_2 desorbed during temperature stabilization period up to 350 °C. Adding this up to the amount of ~ 0.75 wt.% desorbed during the isothermal desorption period of the test at 350 °C (as discussed above) gives us ~ 3.25 wt.% of the total hydrogen desorbed which is still smaller than the total theoretical value of ~ 3.97 wt.% H_2 stored in the $\text{Mg}(\text{AlH}_4)_2 + 2\text{NaCl}$ mixture. We are not sure if this is a pure coincidence but in both cases of Sieverts desorption at 150 and 350 °C, the total amount of hydrogen desorbed in the experiment is short of ~ 0.7 wt.% with respect to the theoretical hydrogen capacity values. Since the calibrated accuracy of desorbed hydrogen capacity is about ± 0.2 wt.% H_2 in our Sieverts-type apparatus (calibrated on a commercial MgH_2) then the experimental deficiency of ~ 0.7 wt.% is not due to the experimental error and as such must be related to some other factor. One explanation could be that the powder synthesized for 5 h already lost about ~ 0.7 wt.% of hydrogen due to partial decomposition of $\text{Mg}(\text{AlH}_4)_2$ during milling. However, this needs further study.

The major problem in the MCAS technology is the formation of a large amount of waste by-product NaCl. With 2 mol of NaCl per only 1 mol of $\text{Mg}(\text{AlH}_4)_2$ (reaction (3)) the excellent theoretical hydrogen capacity ~ 9.3 wt.% of pure $\text{Mg}(\text{AlH}_4)_2$ is reduced to the very inferior theoretical ~ 3.97 wt.% H_2 in the mixture of $\text{Mg}(\text{AlH}_4)_2 + 2\text{NaCl}$. As reported by Mamatha et al. [19] it is possible to separate $\text{Mg}(\text{AlH}_4)_2$ from NaCl by the Soxhlet extraction method which is based on the suspension of the $\text{Mg}(\text{AlH}_4)_2 + 2\text{NaCl}$ mixture in the diethyl ether (Et_2O) solvent. However, there are a couple of serious disadvantages of this extraction method. First, the extracted $\text{Mg}(\text{AlH}_4)_2$ is usually contaminated with the solvent adduct [20]. Second, the extraction process needs several days to be completed and then the

product requires some additional long-time annealing in vacuum [19]. Such a long production time may not be well suited for industrial environment. There is also a problem with the reversibility of the reaction (7). The reactions (7a) and (7b) are reversible producing MgH_2 and Al but still very sluggish [28]. However, our previous studies [15] suggest that the reaction (3) between MgH_2 and Al to form $\text{Mg}(\text{AlH}_4)_2$ is most likely irreversible.

4. Conclusions

A mixture of $\text{Mg}(\text{AlH}_4)_2 + 2\text{NaCl}$ has been successfully synthesized by the mechano-chemical activation synthesis (MCAS) of the stoichiometric mixture of 2NaAlH_4 and MgCl_2 compounds by ball milling for 5 and 10 h in a magneto-mill. The particle size of the as-milled powder mixture is on the order of 2 μm after milling for 5, 10 and 40 h. The $\text{Mg}(\text{AlH}_4)_2$ hydride is nanocrystalline having the grain size of around 18 nm. Even relatively short milling for just 10 h results in a partial decomposition of pre-synthesized $\text{Mg}(\text{AlH}_4)_2$ into $\beta\text{-MgH}_2$ and the nanocrystalline elemental Al (grain size ~ 26 nm). Prolonged milling for 40 h results in a complete decomposition of the $\text{Mg}(\text{AlH}_4)_2$ into nanocrystalline $\beta\text{-MgH}_2$ (grain size ~ 11 nm) and the elemental Al (grain size ~ 20 nm).

DSC test of the $\text{Mg}(\text{AlH}_4)_2 + 2\text{NaCl}$ mixture synthesized for 5 and 10 h, results in the decomposition of $\text{Mg}(\text{AlH}_4)_2$ into $\beta\text{-MgH}_2 + 2\text{Al} + 3\text{H}_2 (+2\text{NaCl})$ within the range 125–180 °C (at the scan rate of 4 °C/min) as confirmed by X-ray diffraction. However, the nature of this transformation being either endothermic [18,19] or exothermic [20] cannot be unambiguously established because a number of samples tested in DSC at the scan rate of 4 and 20 °C/min showed both types of transformation, most likely, owing to a very small enthalpy of decomposition of $\text{Mg}(\text{AlH}_4)_2$, which is cited in the literature as being equal to ~ 1.7 kJ/molH [19]. Desorption experiments of the $\text{Mg}(\text{AlH}_4)_2 + 2\text{NaCl}$ powder synthesized for 5 h, carried out in a Sieverts-type apparatus at 150 °C, show that the total amount of hydrogen desorbed during temperature stabilization period and isothermal desorption period is ~ 2.24 wt.%.

DSC test from 180 to 500 °C of the $\text{Mg}(\text{AlH}_4)_2 + 2\text{NaCl}$ mixture synthesized for 5 and 10 h results in three endothermic reactions with the peak maxima at ~ 271 , ~ 316 and ~ 452 °C (at the scan rate of 4 °C/min). In the first endo effect at ~ 270 °C the $\beta\text{-MgH}_2$ hydride decomposes and the free elemental Mg reacts with the pre-existing free elemental Al forming an equilibrium mixture of intermetallic compound Al_3Mg_2 and Al(Mg) solid solution. The nature of the second peak at ~ 315 °C is not clear and can be interpreted either as due to the formation of the Al_3Mg_2 intermetallic compound or further decomposition of the remnant $\beta\text{-MgH}_2$. Heating of the powder synthesized for 40 h, which contains only a single $\beta\text{-MgH}_2$ hydride results in two endothermic peaks with the maxima at ~ 290 and ~ 451 °C (at the scan rate of 4 °C/min). The former peak is due to the decomposition of $\beta\text{-MgH}_2$. The endo peaks with the maximum at 451–452 °C, observed in all the synthesized powders, are due to the eutectic melting of the mixture of Al_3Mg_2 and Al(Mg) as required by the binary phase diagram Al–Mg. Desorption

experiments on the powder synthesized for 5 h, carried out in a Sieverts-type apparatus at 350 °C (complete decomposition of β -MgH₂), show that the total amount of hydrogen desorbed during temperature stabilization period and isothermal desorption period is ~ 3.25 wt.%. In both cases of Sieverts desorption at 150 and 350 °C, the total amount of hydrogen desorbed in the experiment is short by ~ 0.7 wt.% with respect to the theoretical hydrogen capacity values which one could expect at these respective temperatures. The factor causing such a discrepancy may be related to the prior loss of hydrogen due to partial decomposition of Mg(AlH₄)₂ during ball milling but the exact explanation needs more studies. However, our recent results on the attempts to directly synthesize Mg(AlH₄)₂ from the elemental metals by reactive milling [15] strongly suggests that the reaction (7a) is most likely irreversible.

Acknowledgement

This work was financially supported by a grant from the Natural Sciences and Engineering Research Council of Canada, which is gratefully acknowledged.

References

- [1] J.A. Ritter, A.D. Ebner, J. Wang, R. Zidan, *Mater. Today* (2003) 18–23.
- [2] A. Züttel, P. Wenger, S. Rentsch, P. Sudan, Ph. Mauron, Ch. Emmenegger, *J. Power Sources* 118 (2003) 1–7.
- [3] L. Schlapbach, A. Züttel, *Nature* 414 (2001) 353–358.
- [4] B. Bogdanović, G. Sandrock, *MRS Bull.* 27 (2002) 712–716.
- [5] M. Fichtner, *Adv. Eng. Mater.* 7 (2005) 443–455 (a review).
- [6] E.C. Ashby, R.D. Schwartz, B.D. James, *Inorg. Chem.* 9 (1970) 325–332.
- [7] M. Fichtner, J. Engel, O. Fuhr, O. Kircher, O. Rubner, *Mater. Sci. Eng. B* 108 (2004) 42–47.
- [8] M. Fichtner, O. Fuhr, O. Kircher, *J. Alloys Compd.* 356/357 (2003) 418–422.
- [9] M. Fichtner, O. Fuhr, *J. Alloys Compd.* 345 (2002) 286–296.
- [10] M. Schwarz, A. Haiduc, H. Still, P. Paulus, H. Geerlings, *J. Alloys Compd.* 404–406 (2005) 762–765.
- [11] A. Fossdal, H.W. Brinks, M. Fichtner, B.C. Hauback, *J. Alloys Compd.* 387 (2005) 47–51.
- [12] A. Fossdal, H.W. Brinks, M. Fichtner, B.C. Hauback, *J. Alloys Compd.* 404–406 (2005) 752–756.
- [13] A.M. Seayad, D.M. Antonelli, *Adv. Mater.* 16 (2004) 765–777 (a review).
- [14] A. Zaluska, L. Zaluski, J.O. Ström-Olsen, *J. Alloys Compd.* 288 (1999) 217.
- [15] R.A. Varin, Ch. Chiu, T. Czujko, Z. Wronski, *Nanotechnology* 16 (2005) 2261–2274.
- [16] T.N. Dymova, N.N. Mal'tseva, V.N. Konoplev, A.I. Golovanova, D.P. Alexandrov, A.S. Sizareva, *Russ. J. Coord. Chem.* 29 (2003) 385–389.
- [17] T.N. Dymova, V.N. Konoplev, A.S. Sizareva, D.P. Alexandrov, *Russ. J. Coord. Chem.* 25 (1999) 312–315.
- [18] M. Mamatha, C. Weidenthaler, A. Pommerin, M. Felderhoff, F. Schüth, *J. Alloys Compd.* 416 (2006) 303–314.
- [19] M. Mamatha, B. Bogdanović, M. Felderhoff, A. Pommerin, W. Schmidt, F. Schüth, C. Weidenthaler, *J. Alloys Compd.* 407 (2006) 78–86.
- [20] Y. Kim, E.-K. Lee, J.-H. Shim, Y.W. Cho, K.B. Yoon, *J. Alloys Compd.* 422 (2006) 283–287.
- [21] Calka, A.P. Radlinski, *Mater. Sci. Eng. A* 134 (1991) 1350–1353.
- [22] Patents: WO 9,104,810; US 5,383,615; CA 2,066,740; EP 0,494,899; AU 643,949.
- [23] A. Calka, R.A. Varin, in: T.S. Srivatsan, R.A. Varin, M. Khor (Eds.), *Proceedings of the International Symposium on Processing and Fabrication of Advanced Materials IX (PFAM-IX)*, ASM International, Materials Park, OH, 2001, pp. 263–287.
- [24] H.P. Klug, L. Alexander, *X-ray Diffraction Procedures for Polycrystalline and Amorphous Materials*, John Wiley & Sons, New York, 1974, pp. 618–708.
- [25] R.A. Varin, S. Li, A. Calka, *J. Alloys Compd.* 376 (2004) 222–231.
- [26] R.A. Varin, S. Li, Z. Wronski, O. Morozova, T. Khomenko, *J. Alloys Compd.* 390 (2005) 282–296.
- [27] D.R. Askeland, P.P. Phulé, *The Science and Engineering of Materials*, Thomson Canada Ltd., Toronto, 2006, p. 842.
- [28] M.H. Mintz, Z. Gavra, G. Kimmel, Z. Hadari, *J. Less-common Met.* 74 (1980) 263–270.